Surface Physics Lecture 20.04.2010

Electronic Properties and Surface Electron Spectroscopies: XPS/UPS, Auger and ARPES

XPS: X-ray Photoelectron Spectroscopy
UPS: Ultraviolet Photoelectron Spectroscopy
AES: Auger Electron Spectroscopy
ARPES: Angle-Resolved PhotoEmission Spectroscopy

Dr. Nirmalya Ballav

Paul Scherrer Institute

XPS und UPS

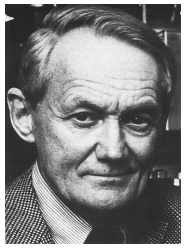

Kai Siegbahn
1918-2007

Die Energie der Photoelektronen liegt im Bereich von 10-2000eV. Demnach ist die Ausdringtiefe im Berich von einigen Monolagen. Werden Röntgen-Strahlen zur Anregung benutzt so wird die Methode **X-ray photoelectron spectroscopy (XPS)** bezeichnet. XPS wurde zum ersten Mal von Kai Siegbahn (Uppsala) 1954 durchgeführt (1981 Nobelpreis). Hierzu wurde ein Energieanalysator entwickelt, der ein Auflösungsvermögen von $\Delta E/E=10^5$ erreicht hat. Wurde auch ESCA (electron spectroscopy for chemical analysis) genannt. XPS ist heute aber gebräuchlicher., weil verschiedene andere elektronenspektroskopiesche Methoden zur chemischen Analyse benutzt werden (z.B. EELS). XPS wird vorallem für die Untersuchung der Rumpfelektronenzustände (core level s pectroscopy) benutzt. Wird ultraviolette Strahlung eingestrahlt so wird von **Ultraviolet Photoelectron spectroscopy (UPS)** gesprochen. UPS wird zur Analyse der Valenzbänder benutzt und wird häufig zur Untersuchung des Bindungscharakters von adsorpierten Molekülen verwendet.

Photonquellen

Aus einem Filament werden Elektronen thermisch emittiert und auf eine Anode Beschleunigt (typ. 20kV). Als Anode wird ein Material verwendet, das über Einen kleinen Bremstrahlungsuntergrund verfügt und eine schamle charakteristische Linienemission hat (möglichst eine dominierende Linie).

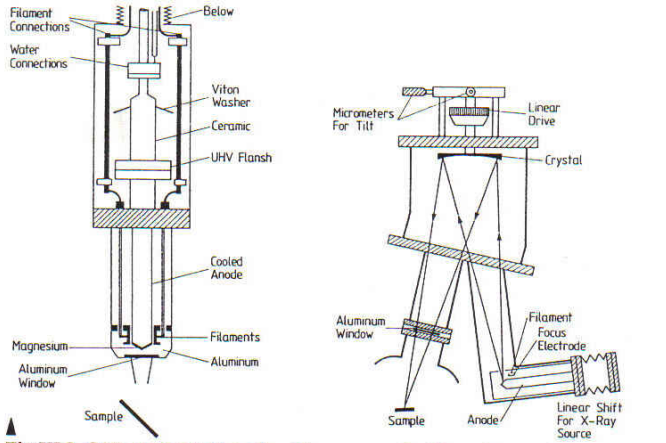

Fig. XI.3. Cross-sectional view of an X-ray source for X-ray Photoemission Spectroscopy (XPS). The anode, composed of either Mg or Al, is water cooled

Fig. XI.4. Schematic of an X-ray monochromator for high-resolution XPS. The X-ray source is flanged to an UHV chamber containing a crystal mirror which acts, by means of Bragg reflection, as a dispersive element

Speziell günstig haben sich Al(1486eV) und Mg(1253eV) erwiesen. Daneben wurden auch Na(1041eV), Si(1739eV) und Y(132,3eV) verwendet, wobei Y einen Speziallfall darstellt, der bereits im Übergansbereich zu UPS liegt. Die Linienbreite ist im Berich von 0.5-1.0eV, sodass Feinstrukturen wie chemische Shifts nur schwer beobachtbar sind. Die Verwendung eines Monochromators ist deshalb notwendig für die Untersuchung der Feinstruktur der „Core levels“

UV-Lampe

Zur Erzeugung von UV-Licht werden Gas-Entladungs-Lampen verwendet.
Diese Lampen sind über differentiell gepumpte Kapillaren mit dem UHV-System verbunden. (gute UV-durchlässige Fenster sind nicht erhältlich). Als besonders günstig hat sich He erwiesen. Je nach Druck ist die He I Linie (1Torr) bzw. die He-II-Linie (0.1Torr) dominant. He I hat eine sehr Intensive Linie bei 21.22eV. Linienbreite: 3-20meV, was die Untersuchung von Feinstrukturen, wie chemical shifts zulässt.

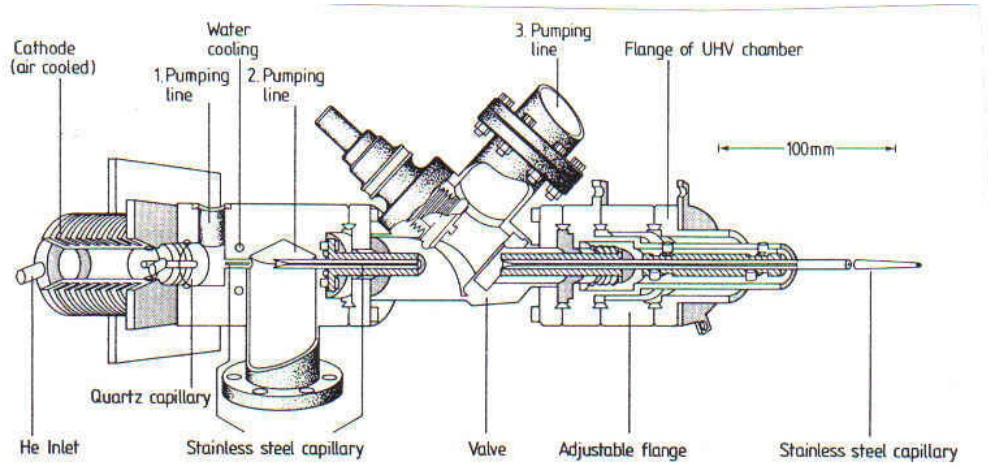

Fig. XI.2. Cross-sectional view of a UV discharge lamp for UV Photoemission Spectroscopy (UPS). The discharge quartz capillary is water cooled; three pump connections allow differential pumping; an UHV valve can interrupt the direct connection between discharge volume and UHV chamber

Zusammenstellung von Photonquellen

Source	Energy [eV]	Relative intensity	Typical intensity at the sample [photons/s]	Linewidth [meV]
He I	21.22	100	$1 \cdot 10^{12}$	3
Satellites	23.09, 23.75, 24.05	< 2 each		
He II	40.82	20*	$2 \cdot 10^{11}$	17
	48.38	2*		
Satellites	51.0, 52.32, 53.00	< 1* each		
Ne I	16.85 and 16.67	100	$8 \cdot 10^{11}$	
Ne II	26.9	20*		
	27.8	10*		
	30.5	3*		
Satellites	34.8, 37.5, 38.0	< 2 each		
Ar I	11.83	100	$6 \cdot 10^{11}$	
	11.62	80÷40*		
Ar II	13.48	16*		
	13.30	10*		
YM_t	132.3	100	$3 \cdot 10^{11}$	450
Mg $K_{\alpha 1,2}$	1253.6	100	$1 \cdot 10^{12}$	680
Satellites $K_{\alpha 3}$	1262.1	9		
$K_{\alpha 4}$	1263.7	5		
Al $K_{\alpha 1,2}$	1486.6	100	$1 \cdot 10^{12}$	830
Satellites $K_{\alpha 3}$	1496.3	7		
$K_{\alpha 4}$	1498.3	3		

Nanojunction-Lab at PSI

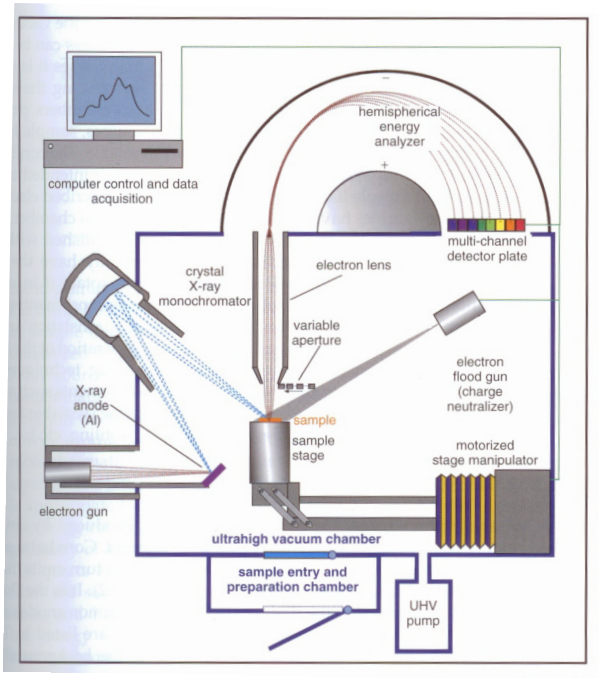

Instrument overview:

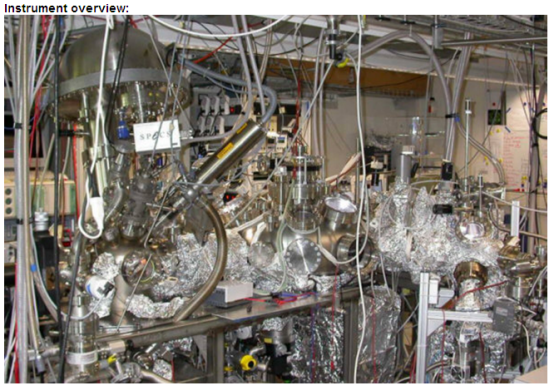

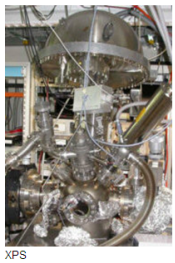

XPS

"UFO" sample exchange chamber

molecule evaporators

XPS: Model

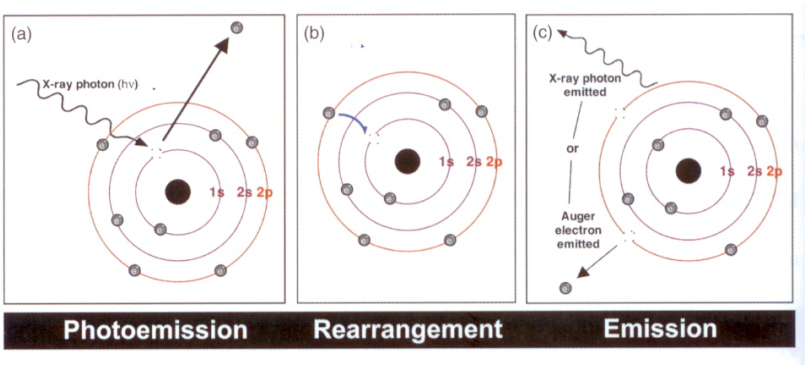

Photoelectron Spectroscopy

Photonen werden eingestrahlt und absorpiert. Die emittierten Photoelektronen werden mittels eines Energieanalysators untersucht (Halbkugel oder 127º-Zylinderanalysator). Die kinetische Energie der Photoelektronen, E_{kin}, hängt von der Photonenergie hν, der Austrittsarbeit Φ und der Bindungsenergie E_b ab.

$$E_{kin} = h\nu - E_b - \phi$$

(Einsteinbeziehung, siehe Photoeffekt)

Damit ergibt das Spektrum der Photoelektronen ein Abbild der Bandstruktur. Als Nullpunkt wird üblicherweise die Fermi-Energie benutzt, welche bei Metallen den Photoelektronen mit höchster Energie entspricht. (Zur Kalibrierung bei Halbleitern und Isolatoren werden auch häufig „Metall-overlayer“ verwendet)

XPS: Core Level Binding Energies

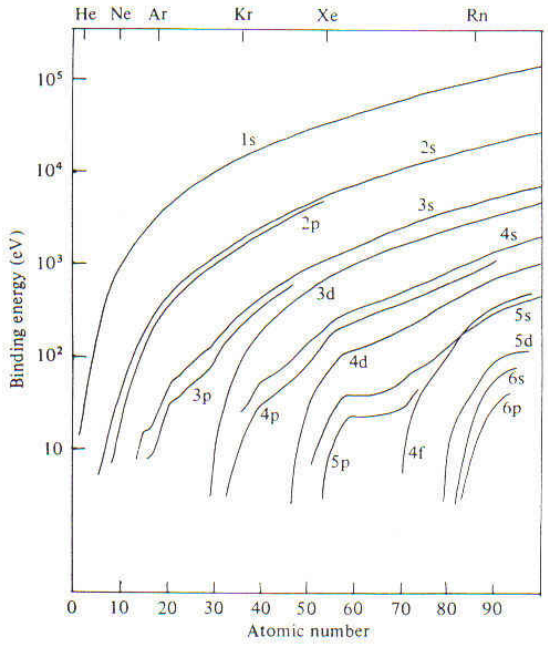

Fig. 3.15 Core electron binding energies of filled levels of the elements. Note that the majority of levels lie below about 10^3 eV and are therefore accessible to conventional laboratory source XPS (from Wertheim (1978) based on the tabulated values of Siegbahn *et al.*, 1967).

XPS: Photoemission Cross-Section

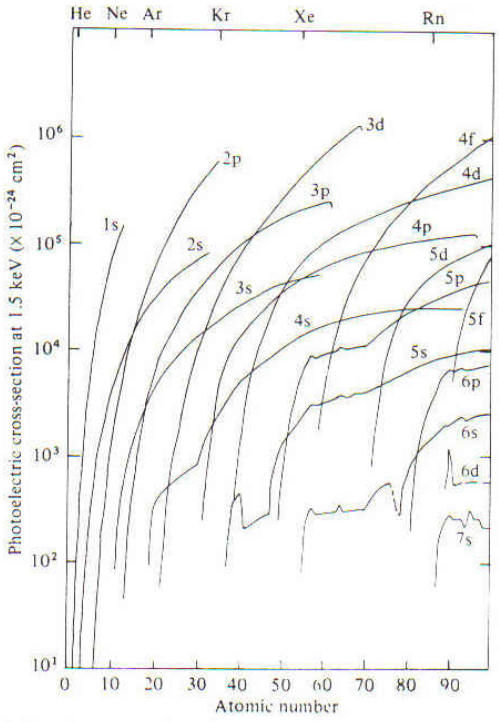

Fig. 3.16 Calculated cross-sections for photoemission from occupied levels of the elements for 1.5 keV photons (from Wertheim (1978) based on the calculated value of Scofield, 1976).

Typisches XPS-Spektra

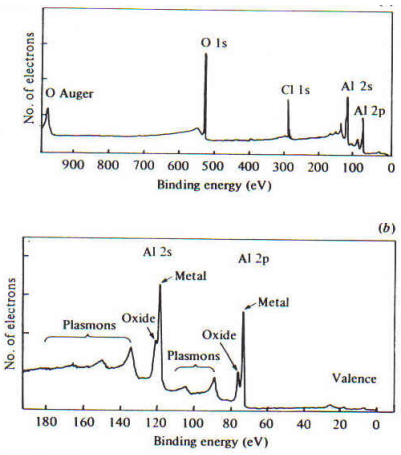

Fig. 3.11 Typical XPS spectra obtained from an oxidised and partly contaminated Al sample taken using monochromatic Al K_α radiation. (*a*) shows the overall features with the main core level emissions labelled. (*b*) shows the low binding energy region on an expanded scale; plasmon loss structure and 'chemically shifted' Al emission lines are labelled (after Fadley, 1978).

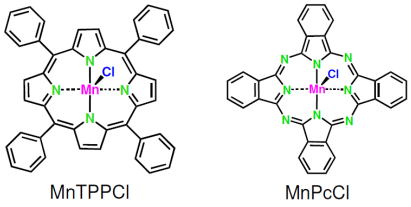

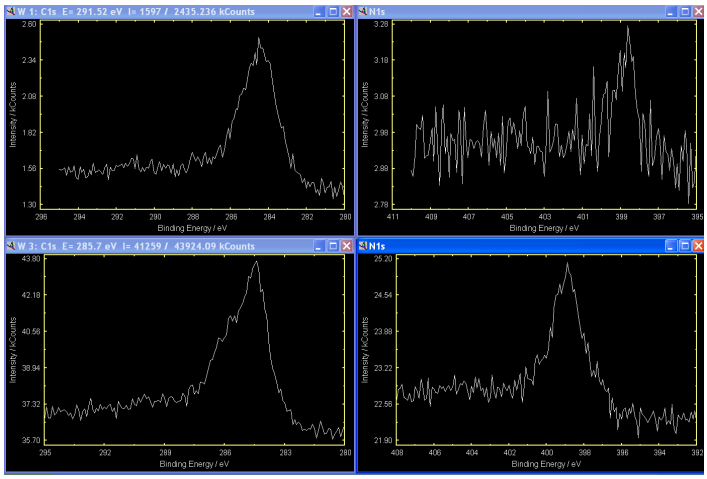

XPS: Spectral Features/ Spin-Orbit Coupling

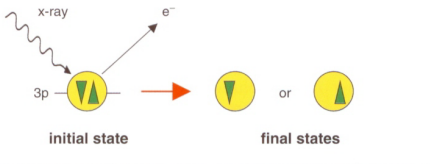

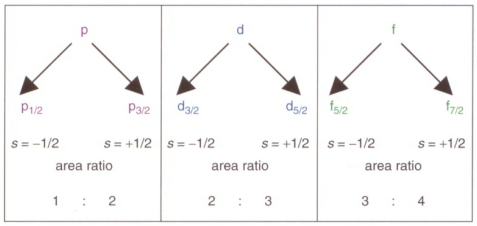

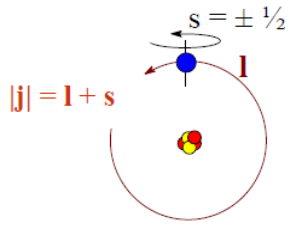

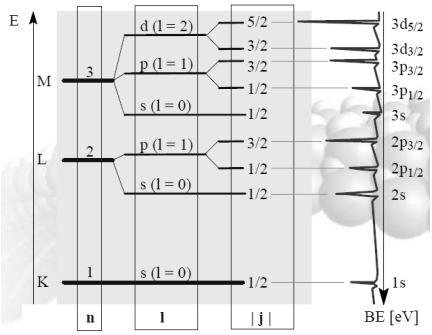

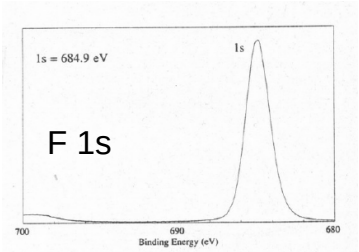

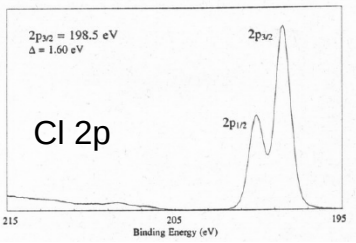

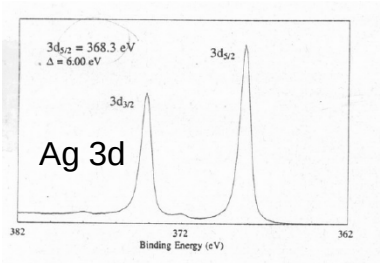

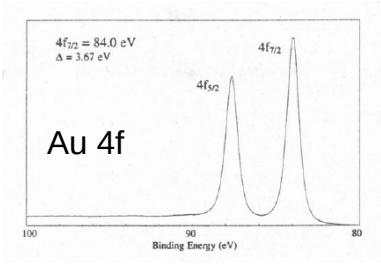

XPS: Chemical Shift

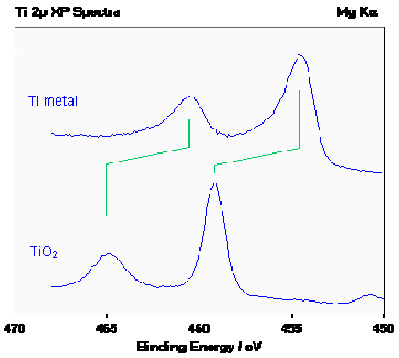

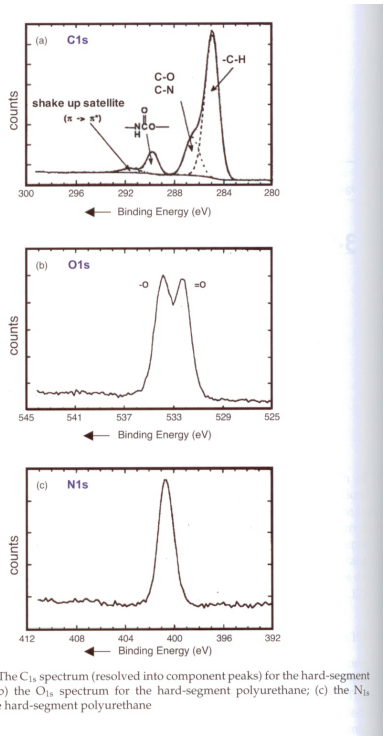

Figure 3.11 (a) The C_{1s} spectrum (resolved into component peaks) for the hard-segment polyurethane; (b) the O_{1s} spectrum for the hard-segment polyurethane; (c) the N_{1s} spectrum for the hard-segment polyurethane

XPS: Layer Thickness

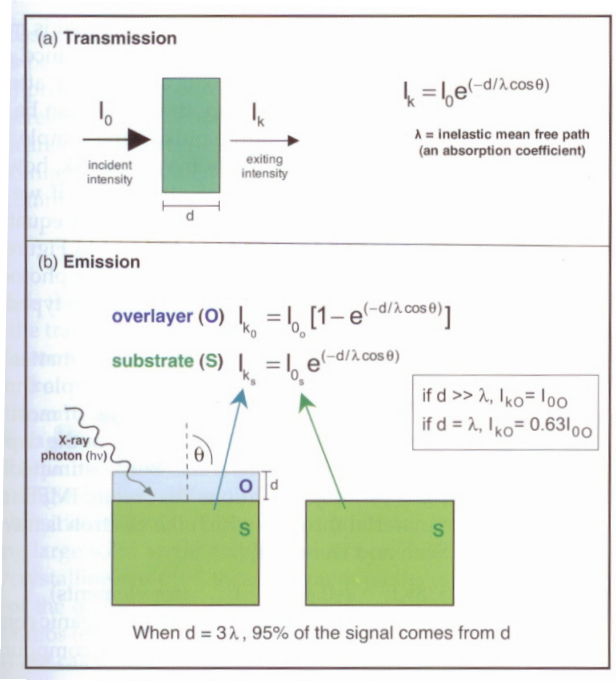

Self-Assembled Monolayers (SAMs)

$I_s \propto e^{-d/\lambda}$ $I_c \propto (1 - e^{-d/\lambda})$

$I_{c/} I_s = A [(1 - e^{-d/\lambda})/e^{-d/\lambda}]$

λ (Å) = 0.3 $(E_{kin})^{0.64}$

DDT/Au ≈ 15Å as reference

XPS: Molecular Packing Density

Sample	Thickness	No. of Atoms	PD
Ref.	√	√	√
Sample X	√	√	√

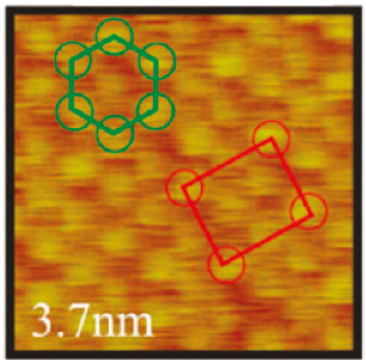

JPC C 2009, 113, 18312

XPS: Depth Profiling

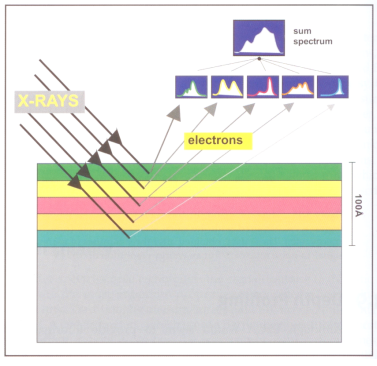

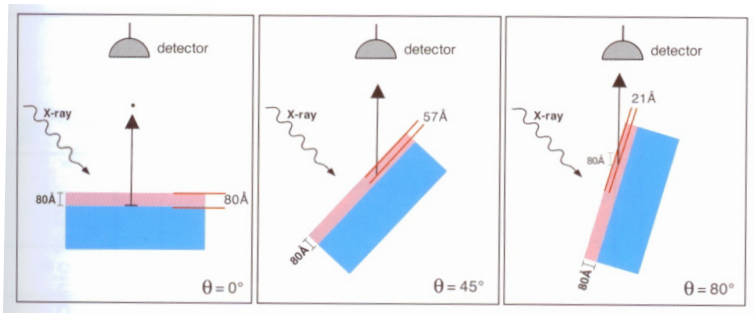

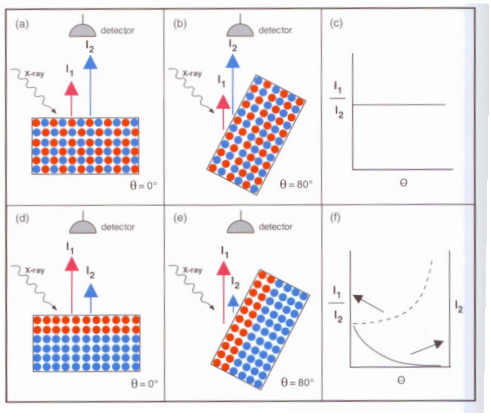

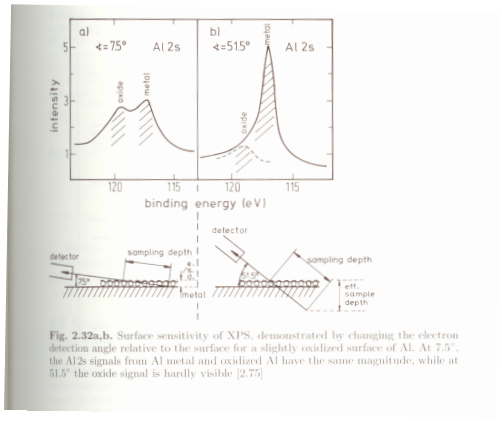

Fig. 2.32a,b. Surface sensitivity of XPS, demonstrated by changing the electron detection angle relative to the surface for a slightly oxidized surface of Al. At 75°, the Al2s signals from Al metal and oxidized Al have the same magnitude, while at 51.5° the oxide signal is hardly visible [2.75]

XPS: Probing Electronic Interaction

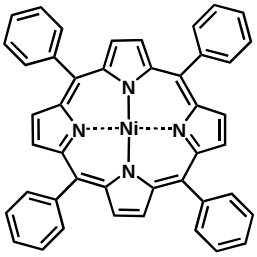

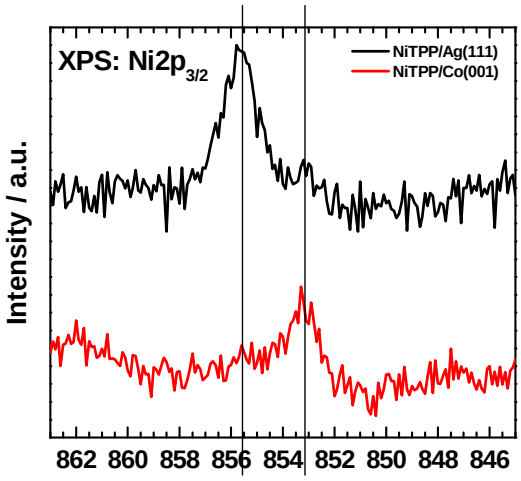

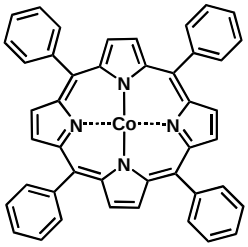

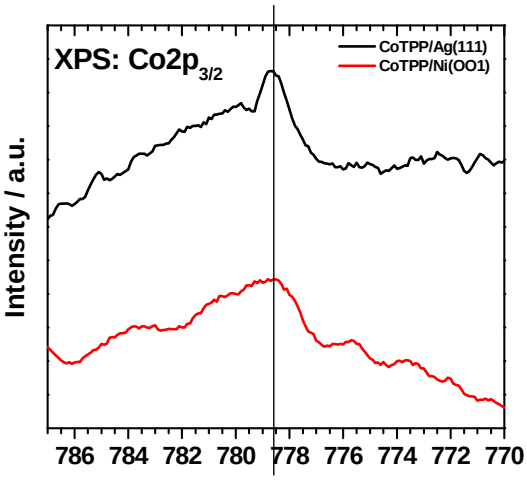

UPS: Probing ϕ and Electronic Interaction

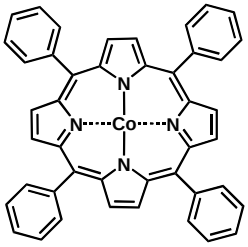

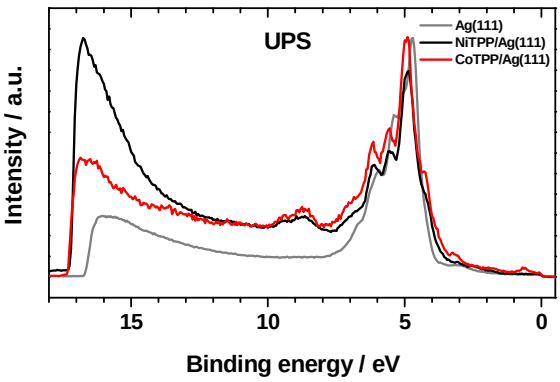

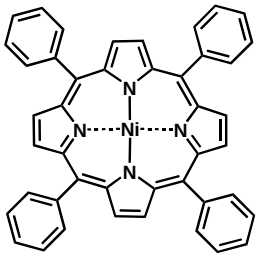

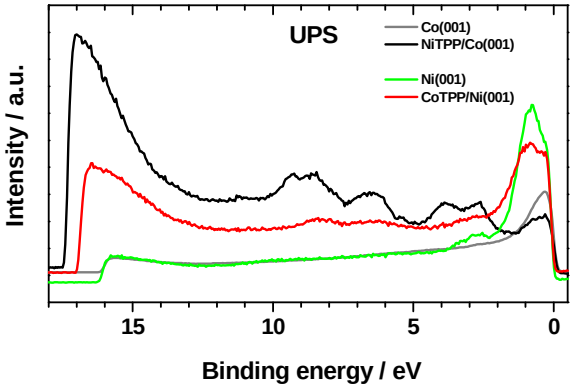

UPS: Probing Electronic Interactions

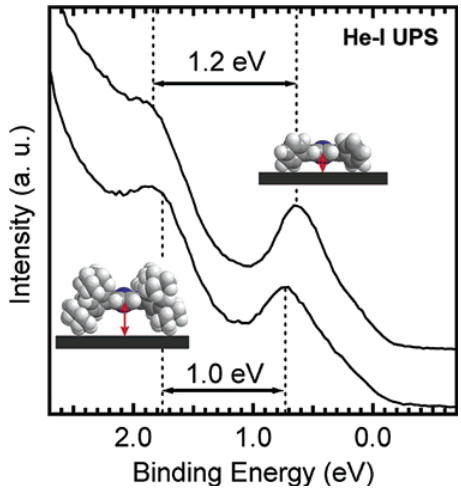

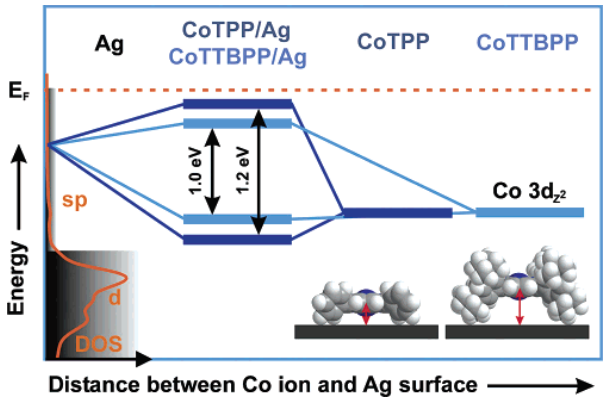

J. Phys. Chem. C 2007, 111, 3090

XPS: Determination of Nitric Oxide

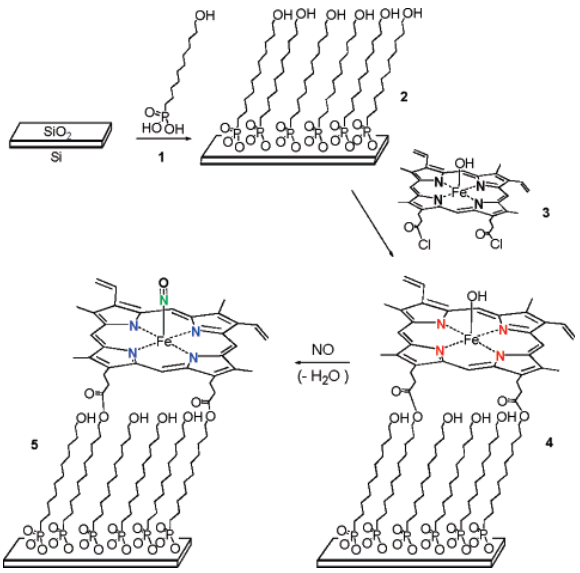

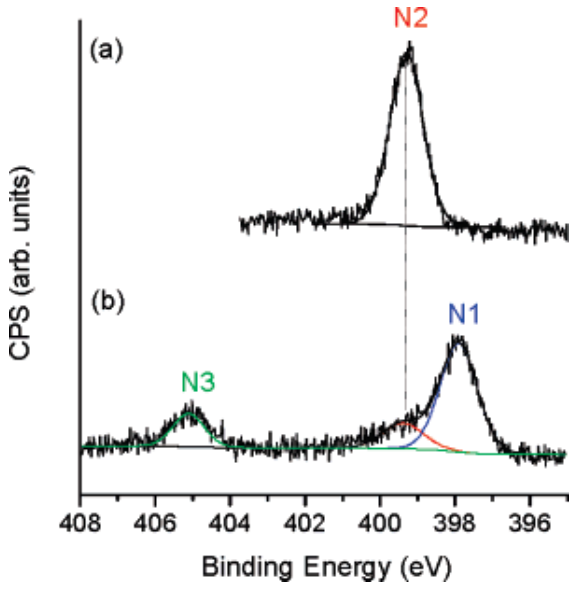

J. Am. Chem. Soc. 2007, 129, 6980

XPS: Monitoring Electronic Interactions

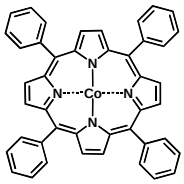

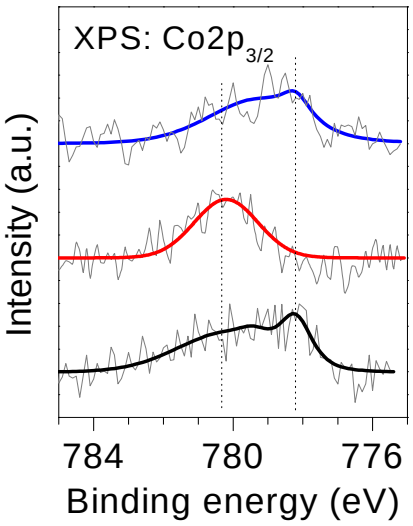

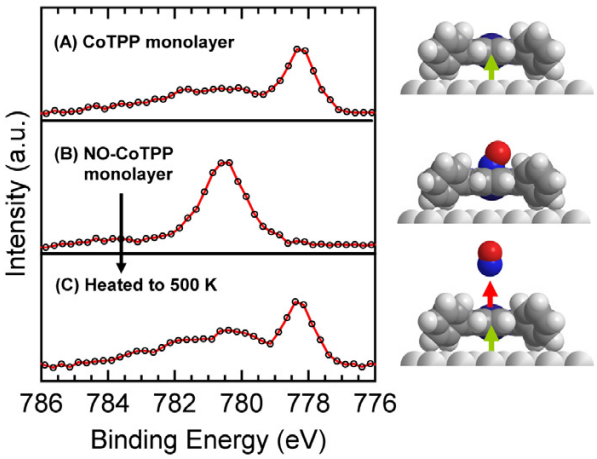

J. Am. Chem. Soc. 2007, 129, 12110

UPS: Monitoring Electronic Interactions

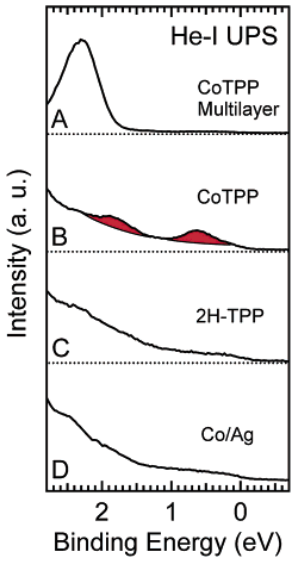

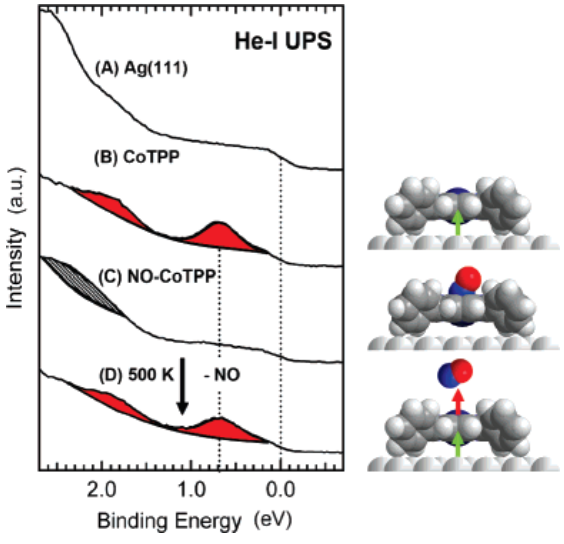

J. Am. Chem. Soc. 2007, 129, 12110

XPS: Catalytic Reactions on Surface

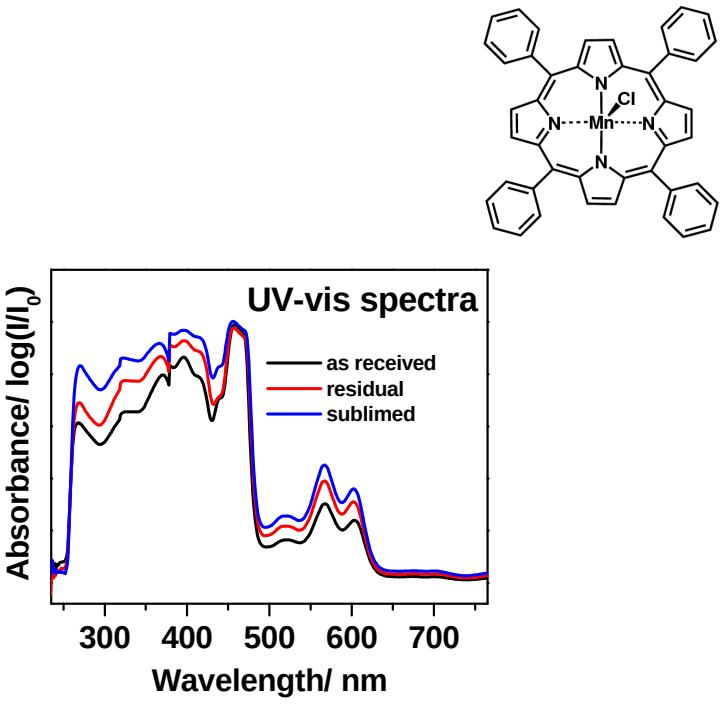

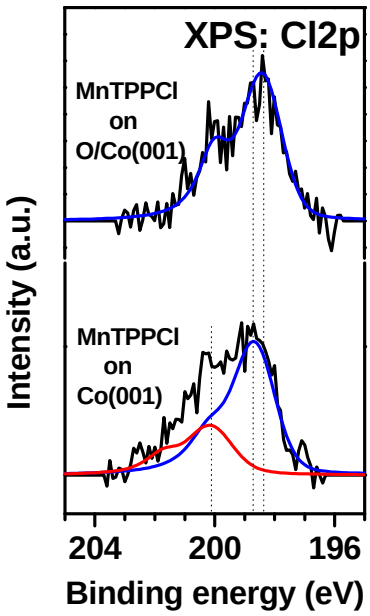

J. Phys. Chem. Lett. 2010 (in press)

XPS: Self-Assembled Monolayers I

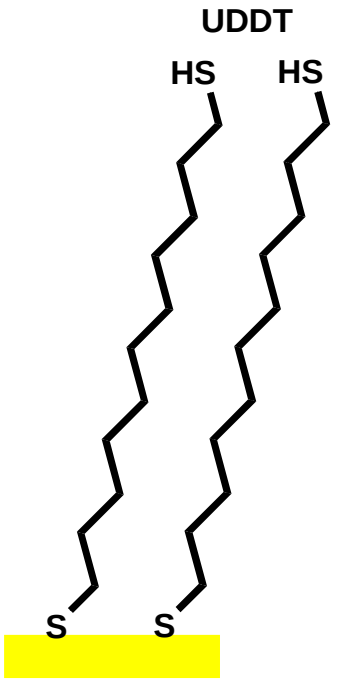

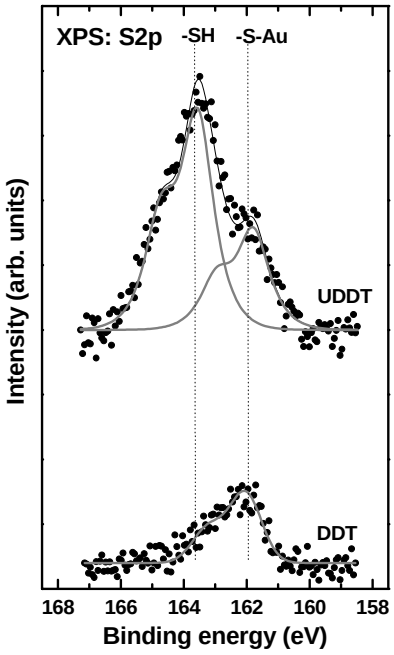

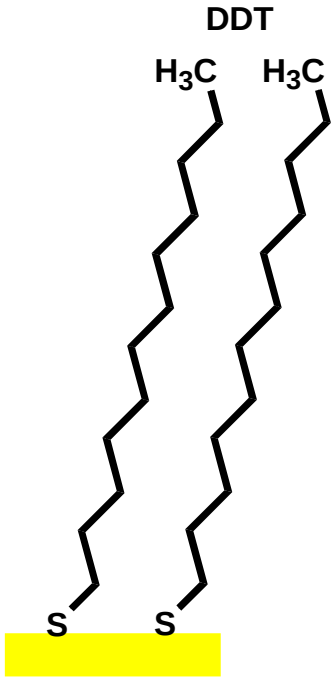

XPS: Self-Assembled Monolayers II

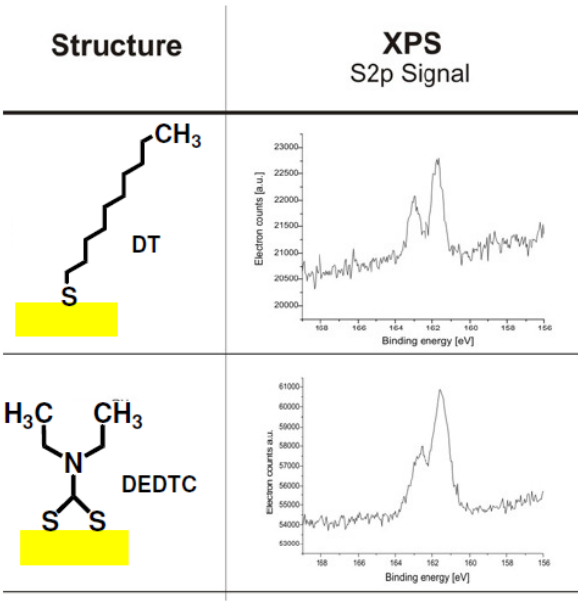

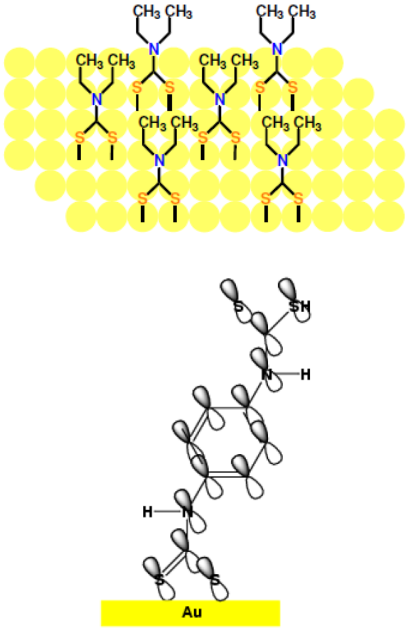

J. Phys. Chem. Lett. 2010, 1, 813

XPS: Probing Molecular Gradients

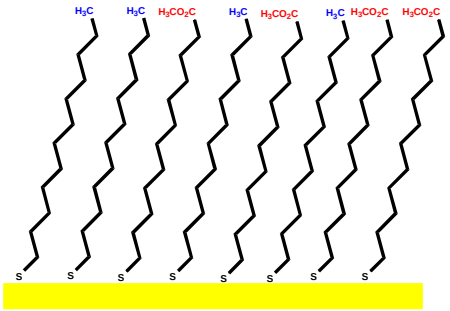

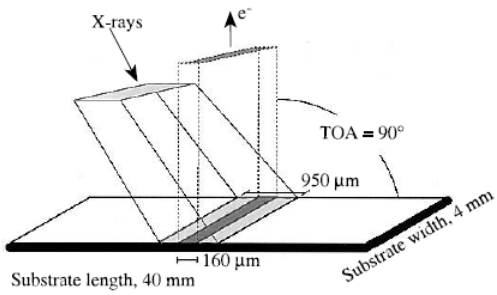

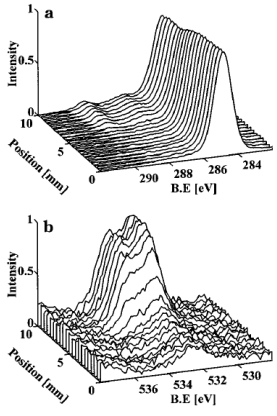

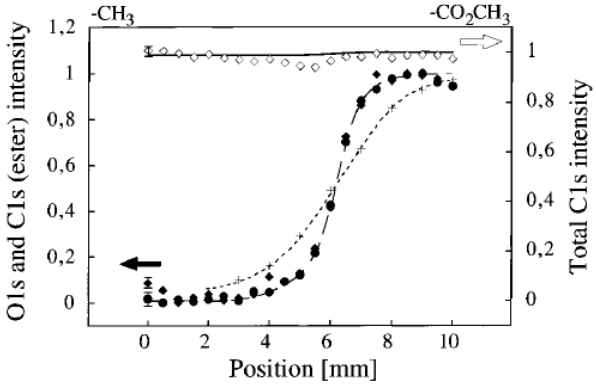

Langmuir 1997, 13, 5329

XPS: Protein Adsorption Study

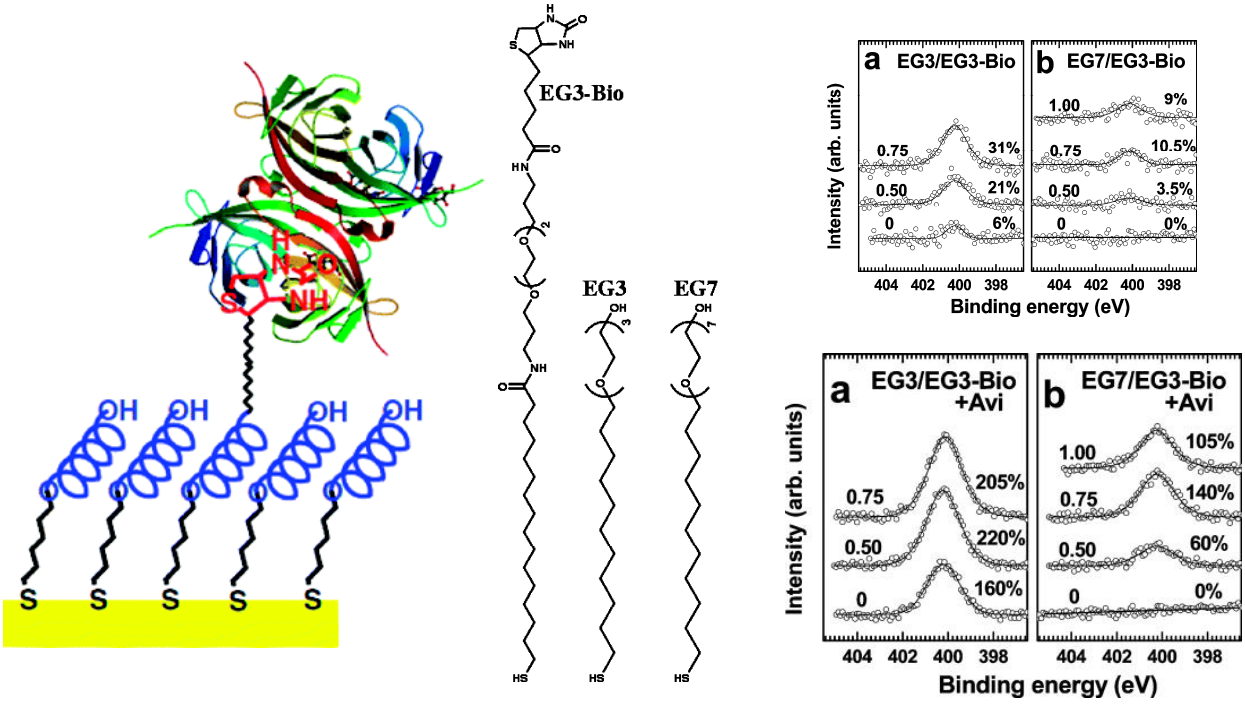

Langmuir 2009, 25, 9189

XPS: Monitoring Electron-Irradiation on SAM

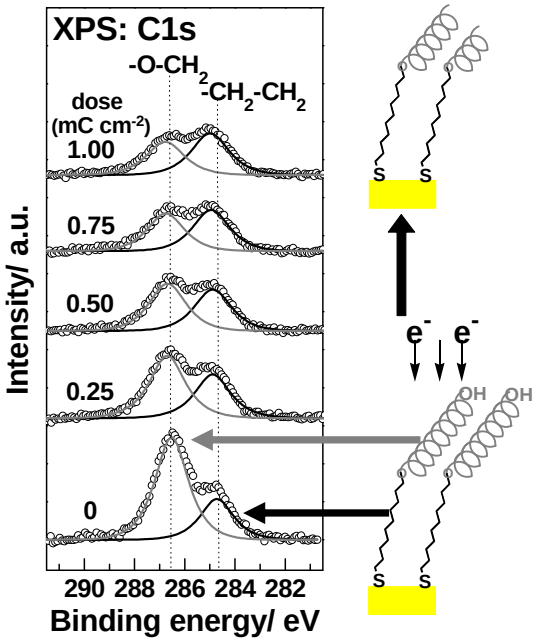

Angew. Chem. Int. Ed. 2009, 48, 5833

XPS: Beam Damage/ Lithography

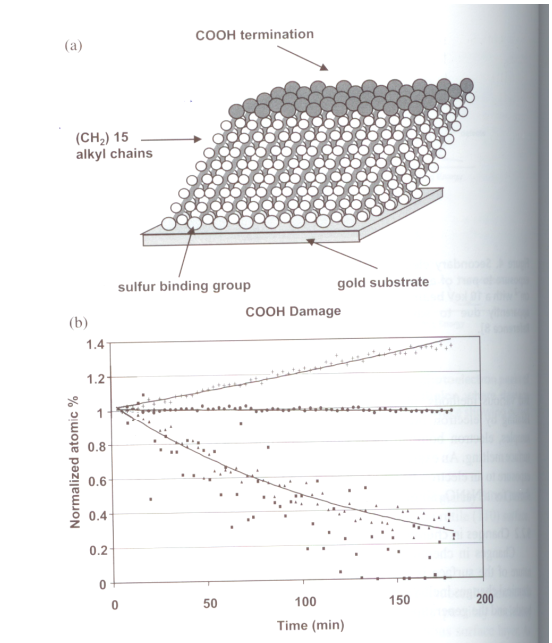

Figure 5. (a) Illustration of a self-assembled monolayer formed on a Au substrate. (b) Normalised atom ratios for a 15-carbon chain self-assembled monolayer terminated with COOH attached to a Au substrate observed as a function of time. Several XPS photoelectron peaks were measured: Au 4f peak [+], C 1s (C–H, C–C) [•], C 1s (C=O) [•] and O 1s [▲]. The most rapid and largest changes are a loss of the O in the COOH termination. The increase in the Au substrate signal is likely due to loss of H from the self-assembled monolayer as the $(CH_2)_{15}$ hydrocarbon chain is damaged. The C 1s (made up of C–H and C–C bonded carbon) peak remains relatively constant, suggesting little loss of C from the CH_2 units in the hydrocarbon chain during the damage. Trend lines are shown for the Au 4f C 1s (C–H, C–C) and O 1s. Because the data for the smaller C 1s (C=O) peak is somewhat noisy no trend line is shown. The data is generally consistent with the O 1s data.

XPS: Imaging

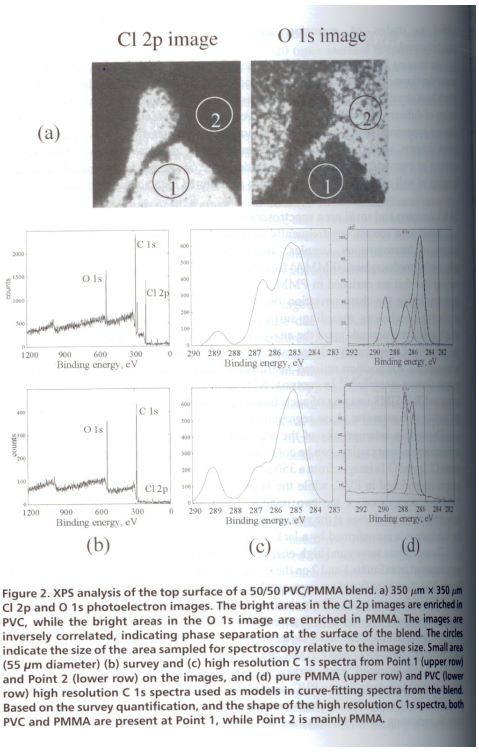

Figure 2. XPS analysis of the top surface of a 50/50 PVC/PMMA blend. a) 350 μm x 350 μm Cl 2p and O 1s photoelectron images. The bright areas in the Cl 2p images are enriched in PVC, while the bright areas in the O 1s image are enriched in PMMA. The images are inversely correlated, indicating phase separation at the surface of the blend. The circles indicate the size of the area sampled for spectroscopy relative to the image size. Small area (55 μm diameter) (b) survey and (c) high resolution C 1s spectra from Point 1 (upper row) and Point 2 (lower row) on the images, and (d) pure PMMA (upper row) and PVC (lower row) high resolution C 1s spectra used as models in curve-fitting spectra from the blend. Based on the survey quantification, and the shape of the high resolution C 1s spectra, both PVC and PMMA are present at Point 1, while Point 2 is mainly PMMA.

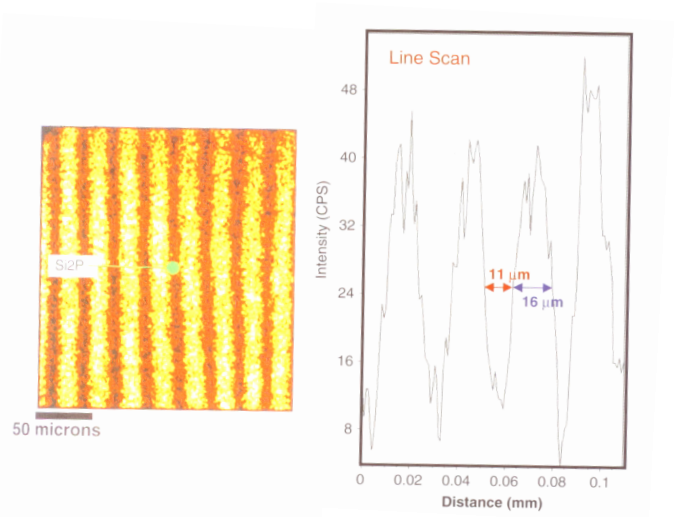

Auger Electron Spectroscopy (AES)

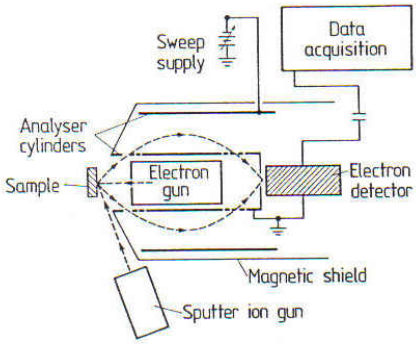

Fig. III.3. Schematic plot of a standard experimental set-up for Auger Electron Spectroscopy (AES). The primary electron beam is generated by an electron gun which is integrated on the central axis of a Cylindrical Mirror Analyser (CMA). An additional sputter ion gun provides the possibility of depth analysis

Das Primärelektron wechselwirkt mit der Oberfläche und erzeugt ein Augerelektron, welches ein Abbild der Rumpfelektronenbindungsenergien ist. Es handelt sich um eine Rumpfelektronenspektroskopie.
(core level spectroscopy).

Elektronenkanone:2000-5000eV
CMA-Energieanalysator, Retarding field analysator oder Halbkugelanalysator
Bei gewissen CMA-Analysatoren ist e-Kanone integriert, was für Tiefenprofilanalyse von Vorteil ist (Kombination mit „ion sputtering“)

Auger-prozess

Der Augerprozess wird in 3 Etappen eingeteilt:
1) Das Primärelektron erzeugt ein Loch in einem Rumpfelektronenzustand (K oder L-Schale) mittels Ionisation.
2)Das Loch wird durch ein Elektron aus einer höheren Schale aufgefüllt (filling process).
3) Die Energie welche in 2 gewonnen wurde, wird auf Elektron der gleichen oder einer verschiedenen Schale übertragen, welches dann ausgesandt wird. Das Augerelektron hat eine charakteristische Energie, was zur Elementanalyse verwendet wird.

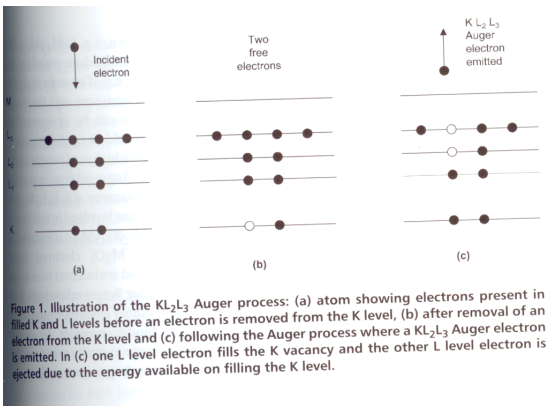

Figure 1. Illustration of the KL_2L_3 Auger process: (a) atom showing electrons present in filled K and L levels before an electron is removed from the K level, (b) after removal of an electron from the K level and (c) following the Auger process where a KL_2L_3 Auger electron is emitted. In (c) one L level electron fills the K vacancy and the other L level electron is ejected due to the energy available on filling the K level.

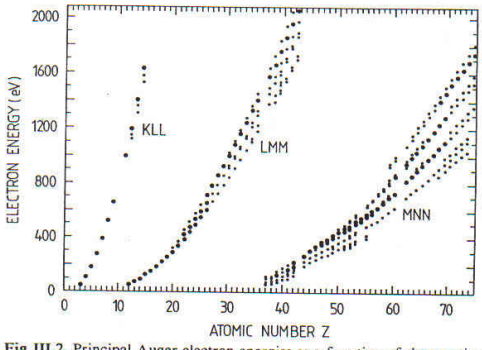

Fig. III.2. Principal Auger electron energies as a function of the atomic number Z. The strongest transitions of each element are indicated by bold points [III.2]

Typisches AES-Spectra

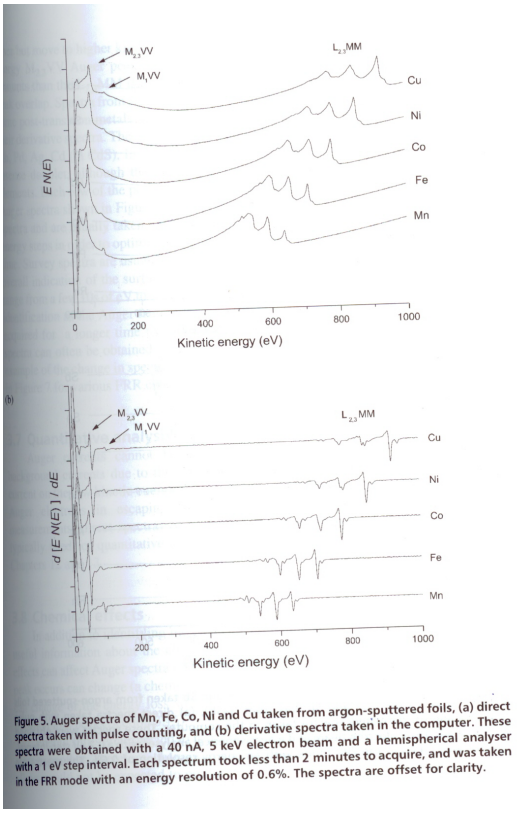

Figure 5. Auger spectra of Mn, Fe, Co, Ni and Cu taken from argon-sputtered foils, (a) direct spectra taken with pulse counting, and (b) derivative spectra taken in the computer. These spectra were obtained with a 40 nA, 5 keV electron beam and a hemispherical analyser with a 1 eV step interval. Each spectrum took less than 2 minutes to acquire, and was taken in the FRR mode with an energy resolution of 0.6%. The spectra are offset for clarity.

PhotoEmission Spectroscopy

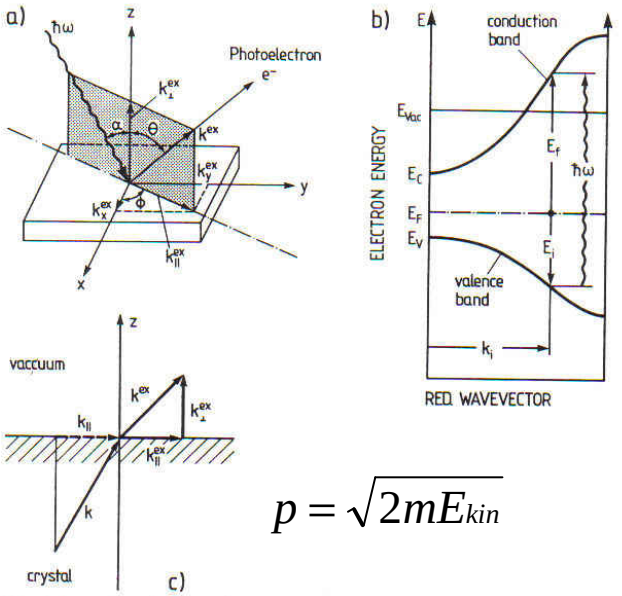

$$p = \sqrt{2mE_{kin}}$$

Fig.6.6a–c. Description of a photoemission experiment. (a) Definition of the angles and wave vectors of the incident photon ($\hbar\omega$) and emitted electron (e^-). (b) Representation of the photoexcitation process in the electronic band scheme E($\mathbf{k}$) of a semiconductor. Only direct transitions with $\mathbf{k}_i \simeq \mathbf{k}_f$ are taken into account. The energies of the initial state (E_i) and final state (E_f) are referred to the Fermi level E_F. (c) Conservation of the wave vector component $\mathbf{k}_\parallel$ (parallel to the surface) upon transmission of the emitted electron through the surface

PES: Band-Structure ans Surface State

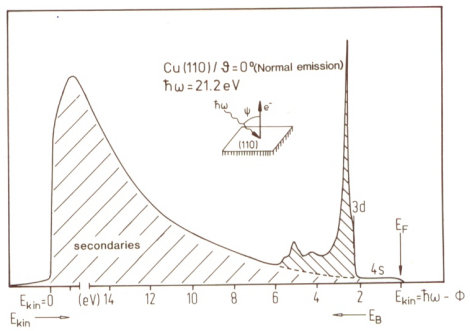

Fig. 1.7. UPS (HeI, $\hbar\omega = 21.2\,\mathrm{eV}$) spectrum from a (110) face of Cu (normal emission, $\vartheta = 0$, ϑ being the polar angle with respect to the surface normal). The flat 4s band and the structured 3d band are seen. The cutoff marks the point where $E_{\mathrm{kin}} = 0$ and via (1.2) the work function can then be derived

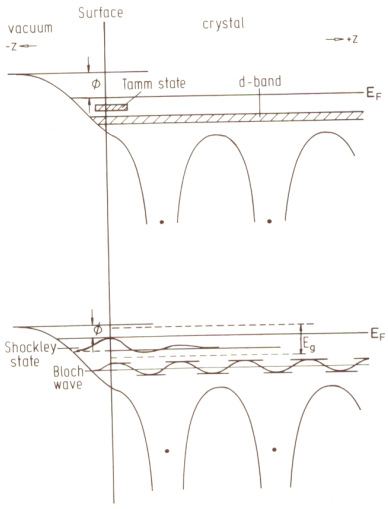

Fig. 8.4. Tamm and Shockley states. The Tamm state (*top*) is split-off from a band (e.g., a d band) of the crystal by the change in potential at the surface. A Shockley state (*bottom*) is a state created in a gap of the bulk-band structure due to the termination of the crystal by a surface (semi-infinite crystal)

PES: Surface State

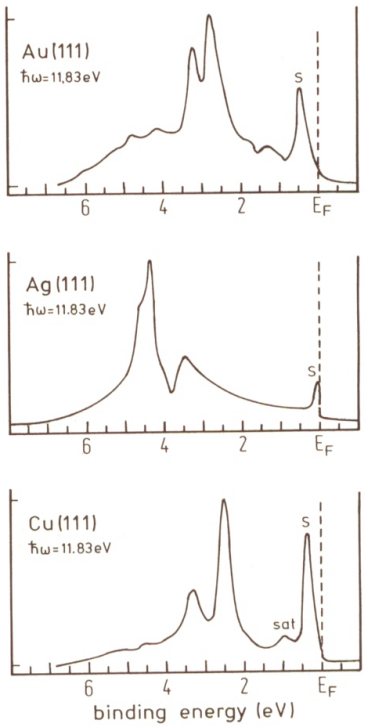

Fig. 8.7. UPS spectra of the (111) surfaces of Cu, Ag and Au with $\hbar\omega = 11.83\,\mathrm{eV}$. For all three metals a surface state (label S) is observed near E_F in the so-called L-gap at $E_F \leq E_S \leq 1\,\mathrm{eV}$, see Fig. 8.6 [8.24]

Angle Resolved PhotoEmission Spectroscopy

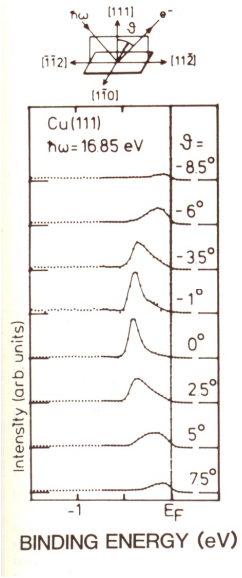

Fig. 8.8. Measurement of the dispersion of the L-gap surface state for Cu(111) (near normal emission, $\hbar\omega = 16.85\,\text{eV}$) The emission direction is in a (110) plane and it is tilted towards [1̄12] and [112]. In going away from the normal the surface state disperses towards the Fermi energy. The $\vartheta = 0$ energy is the same as in Fig. 8.7, ($\hbar\omega = 11.83\,\text{eV}$), indicating that one is indeed observing a surface state. Note that the contribution of the satellite of the NeI radiation to the spectra has been subtracted from the measured experimental data [8.25]

Winkelaufgelöste Messungen, erlauben die Bestimmung der Oberflächen-Bandstruktur. Ferner können Oberflächenzustände von Bulk-Zuständen Unterschieden werden. Oberflächenzustände hängen nicht von $k_\perp$ ab und fallen oft in ein Gap der Bulkzustände.

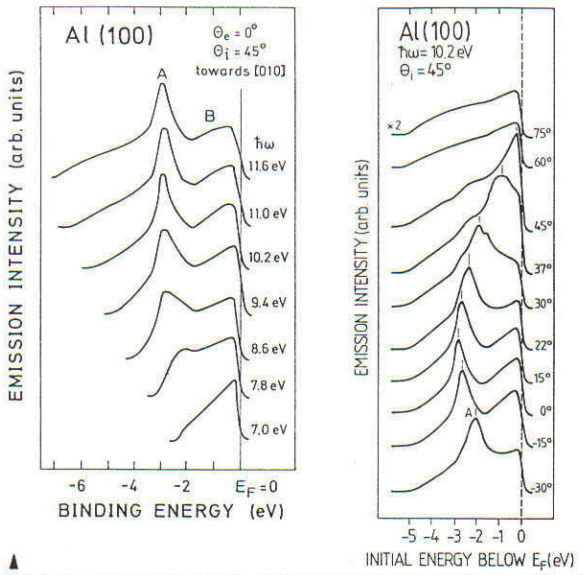

Fig.6.12. Experimental spectra of photoelectrons emitted normal to the Al(100) surface for photon energies between 7 and 11.6 eV (direction of incidence 45° to the [011] direction) [6.12]

Fig.6.13. Photoemission spectra from the Al(100) surface with different polar angles in the (011) plane; photon energy $\hbar\omega = 10.2$ eV, direction of incidence 45° to the [011] direction [6.12]

ARPES: Surface States

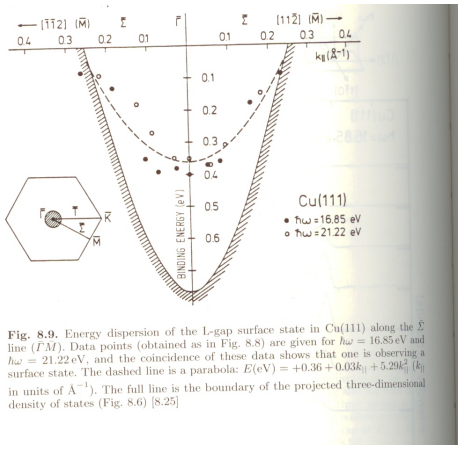

Fig. 8.9. Energy dispersion of the L-gap surface state in Cu(111) along the $\bar{\Sigma}$ line ($\bar{\Gamma}\bar{M}$). Data points (obtained as in Fig. 8.8) are given for $\hbar\omega = 16.85\,\text{eV}$ and $\hbar\omega = 21.22\,\text{eV}$, and the coincidence of these data shows that one is observing a surface state. The dashed line is a parabola: $E(\text{eV}) = +0.36 + 0.03k_{\parallel} + 5.29k_{\parallel}^2$ ($k_{\parallel}$ in units of Å^{-1}). The full line is the boundary of the projected three-dimensional density of states (Fig. 8.6) [8.25]

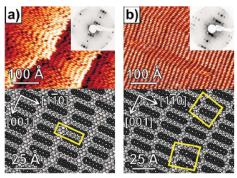

FIG. 1. (Color online) Observed adlayer structures for submonolayer and monolayer coverages of pentacene on Cu(110): (a) 0.8 ML; (b) 1.0 ML. Top: STM images 30×40 nm². Insets: corresponding LEED patterns taken at (a) 53.5 and (b) 63.0 eV. Bottom: structural models with unit cells marked in pale gray (yellow).

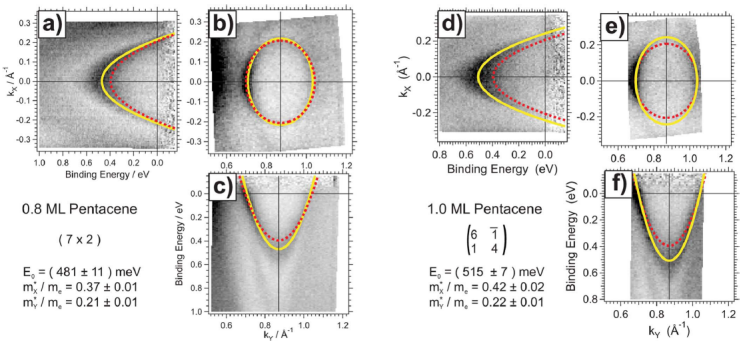

FIG. 3. (Color online) Dispersion of the $\bar{Y}$ surface state of a Cu(110) surface, covered with (a)–(c) 0.8 ML pentacene and (d)–(f) 1.0 ML pentacene. The straight lines marked in pale gray (yellow) mark the fit of a paraboloid to the experimental data. The dotted lines marked in gray (red) correspond to the paraboloid fitted to the experimental data of the clean Cu(110) surface from Fig. 2.

Phys. Rev. B 2009, 325, 300

ARPES: Coupled Quantum Dots from Nanoporous Network on Cu(111)

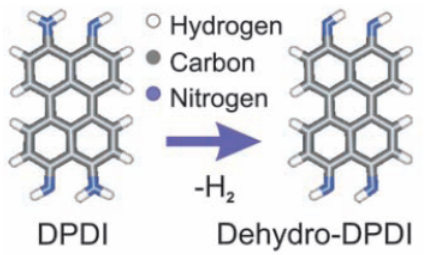

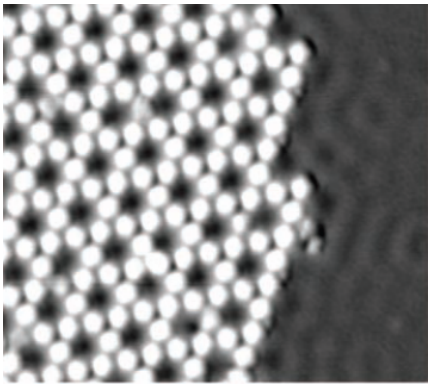

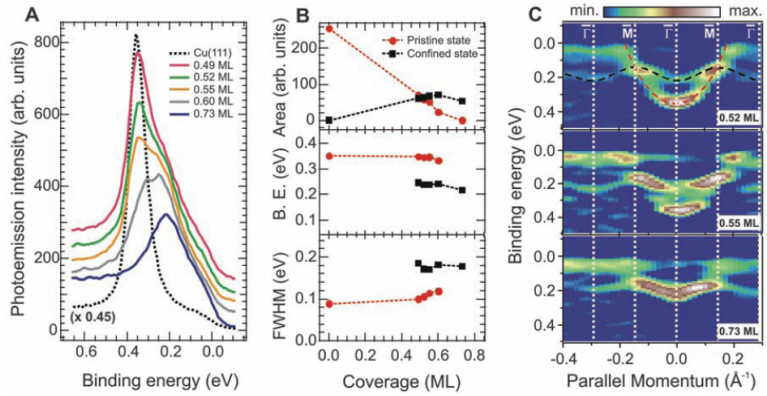

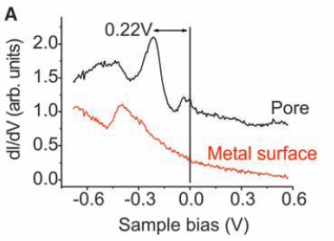

Science 2009, 325, 300

IPES: Inverse PhotoElectron Spectroscopy

Bestimmung der Zustandsdichte der unbesetzten Zustände. Einstrahlung von Elektronen und Messung von Photonen. Zwei Moden: 1. Bremstrahlenspektroskopie: Konstante Elektronenenergie, energieaufgelöste Messung des Lichtes. 2. Isochromate spectroscopy: Elektronenenergie wird variiert. Nur Licht aus einem bestimmten Wellenlängenbereich wird gemessen. Spezieller Bandpassfilter (CaF_2 oder SrF_2-Fenster kombiniert mit Geiger-Zähler mit He gefüllt, sowie einigen J-Kristallen). Vorteil: Grosser Akzeptanzwinkel.

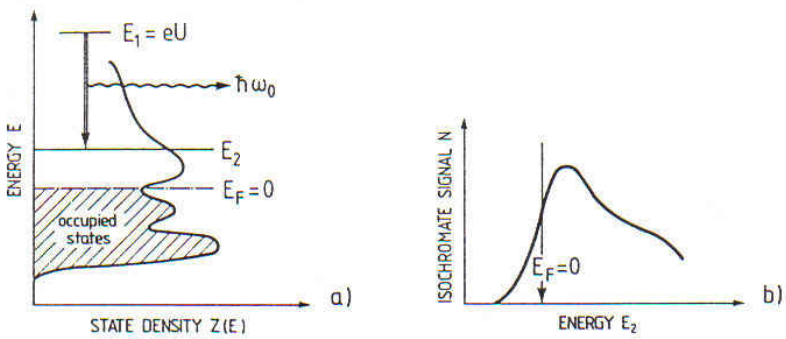

Fig. XI.6. (a) Schematic representation of the inverse photoemission process. An electron injected from outside the crystal enters an excited electronic state E_1 (=eU if an external voltage U accelerates the electrons onto the sample); the electron is deexcited into a state E_2 and the corresponding energy is emitted as a photon of energy $\hbar\omega_0 = E_1 - E_2$. (b) Schematic isochromate spectrum $N(E_2) \propto Z(E_2)$ as obtained according to (a)

IPES of Cu(100)

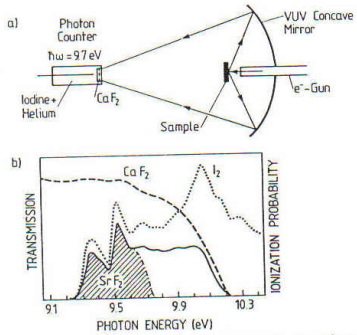

Fig. XI.7. (a) Inverse photoemission set-up using a Geiger counter (isochromate spectroscopy). The UV radiation emitted from the sample is focussed onto the window of a Geiger photon counter. (b) The spectral window of the detector is determined by the spectral transmittance of the counter window (SrF_2 or CaF_2) and by the spectral dependence of the ionization process of iodine [XI.5, 6]

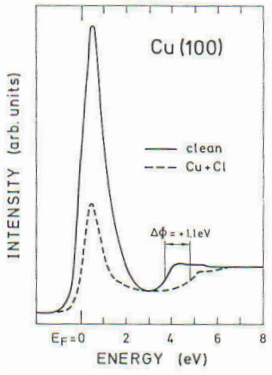

Fig.6.28. Inverse photoemission (isochromate) spectrum on a Cu(100) surface, clean (*full line*) and after adsorption of chlorine (*broken line*). The energy scale extends from the Fermi level E_F up towards the vacuum level [6.27]

Summary: PES and IPES

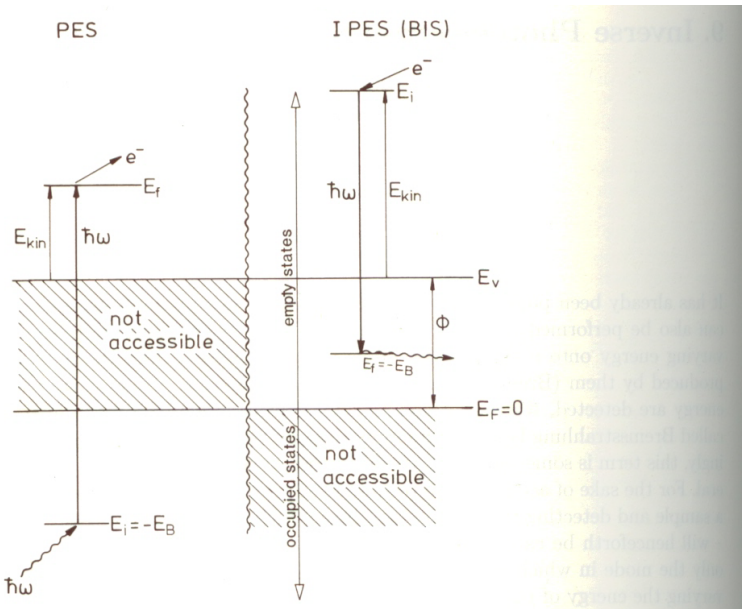

Fig. 9.1. Schematic diagram of PhotoEmission Spectroscopy (PES) and Inverse PhotoEmission Spectroscopy (IPES). In PES the energy range between the Fermi energy and the vacuum level is not accessible, while in IPES the unaccessible range is that below E_F. Thus the two techniques complement each other

Further Reading

1. **Surface Analysis** by Vickermann and Gilmore (Eds)
2. **Photoelectron Spectroscopy** by Huefner
3. **Surface Analysis by Auger and XPS** by Briggs and Grant (Eds.)